

This is an Open Access document downloaded from ORCA, Cardiff University's institutional repository:<https://orca.cardiff.ac.uk/id/eprint/105799/>

This is the author's version of a work that was submitted to / accepted for publication.

Citation for final published version:

Demchenko, Iraida N., Melikhov, Yevgen , Syryanyy, Yevgen, Zaytseva, Irina, Konstantynov, Pavlo and Chernyshova, Maryna 2018. Effect of argon sputtering on XPS depth-profiling results of Si/Nb/Si. *Journal of Electron Spectroscopy and Related Phenomena* 224 , pp. 17-22. 10.1016/j.elspec.2017.09.009

Publishers page: <https://doi.org/10.1016/j.elspec.2017.09.009>

Please note:

Changes made as a result of publishing processes such as copy-editing, formatting and page numbers may not be reflected in this version. For the definitive version of this publication, please refer to the published source. You are advised to consult the publisher's version if you wish to cite this paper.

This version is being made available in accordance with publisher policies. See <http://orca.cf.ac.uk/policies.html> for usage policies. Copyright and moral rights for publications made available in ORCA are retained by the copyright holders.



Effect of Argon Sputtering on XPS Depth-Profiling Results of Si/Nb/Si

Iraida N. Demchenko^{a,*}, *Yevgen Melikhov*^{a,b}, *Yevgen Syryanyy*^a, *Irina Zaytseva*^a,
Pavlo Konstantynov^a, and *Maryna Chernyshova*^c

^a Institute of Physics PAS, Lotnikow Alley 32/46, 02-668 Warsaw, Poland

^b Cardiff University, Newport Rd., Cardiff, CF24 3AA, U.K.

^c Institute of Plasma Physics and Laser Microfusion, Hery Street 23, 01-497 Warsaw, Poland

* *Corresponding author: demch@ifpan.edu.pl*

Abstract

Ultrathin Si/Nb/Si trilayer is an excellent example of a system for which dimensionality effects, together with other factors like type of a substrate material and growth method, influence strongly its superconducting properties. This study offers some important insights into experimental investigation of density of states of such a system with the aim to identify an electronic structure of the interface as a function of niobium layer thickness. For that, two Si/Nb/Si trilayers with 9.5 and 1.3 nm thick niobium layer buried in amorphous silicon were studied using high-resolution (HR) XPS depth-profile techniques. Strong influence of sputtering was observed, which resulted in severe intermixture of Si and Nb atoms. Nevertheless, a sharp top interface and metallic phase of niobium were detected for the thicker layer sample. On the contrary, a Nb-rich mixed alloy at top interface was observed for the thinner layer sample.

Keywords

High-resolution X-ray photoelectron spectroscopy, XPS, Si/Nb/Si, NbSi, depth profiling

1. Introduction

The reduction of the thickness of superconducting films increases the disorder and leads eventually to the thickness-induced superconductor–insulator transition. In addition, this transition may also be induced by the external magnetic field. This evolution remains one of the most important and complex problems in condensed matter physics [1]. Previously it was confirmed that film thickness, substrate material, growth method and conditions strongly influence superconducting properties and study of these effects inevitably lead to deeper knowledge on the subject [2-13].

In that context, ultrathin Si/Nb/Si trilayers prepared by magnetron sputtering are a nice example of such a system. Recent investigations confirmed that critical temperature decreases with decrease of niobium thickness until it totally disappears at ~ 1.2 nm. At the same time, the structure in this system changes from crystalline above ~ 5 nm to amorphous below ~ 3.3 nm [14, 15]. In addition, a change of the Hall coefficient sign from positive to negative was revealed occurring at ~ 1.6 nm. The change of the sign can be interpreted by presence of two types of carriers contributing to the conductivity of the layers: holes and electrons. As in bulk niobium, the hole contribution dominates the transport in thicker samples, however, the electron contribution becomes increasingly important with decrease of the thickness of the Nb layer. Nevertheless, further studies are required to identify the correct reason(s) for the electron distribution and experimental investigation of density of states is the most suitable for this purpose.

In this paper, we study the electronic states of Nb and Si at the surface and in depth of ultrathin Si/Nb/Si trilayers by means of depth-profiling X-ray Photoelectron Spectroscopy (XPS). Usefulness of this technique was shown by investigations of electronic structure near the Fermi level for amorphous [16-19] and crystalline $\text{Nb}_{1-x}\text{Si}_x$ [20]. Despite this, there are a number of reports where authors note that interpretation of XPS data recorded in combination with argon sputtering procedure should be performed with special care as sputtering itself can seriously affect the interlayer structure. One has to remember that ion sputtering, even if noble gas ions are used, generates a large number of artifacts in subsurface region. Some of the examples of artifacts are atomic mixing and knock-on implantation, preferential sputtering, bond breaking, phase formation, segregation, radiation-enhanced diffusion, roughness formation, and others. Such effects have been studied over the last decades and critical reviews of their influences on surface analytical techniques were published [21-24]. Interpretation of XPS data presented in this work was done taking into account some of these effects.

2. Experimental details

The trilayers under study were grown on glass substrates by magnetron sputtering in the high-vacuum chamber at room temperature. Two samples were grown with the thickness of niobium layer being 9.5 nm (referred as 'the thicker layer sample') and 1.3 nm ('the thinner layer sample'). The thickness of top and bottom silicon layers was 10 nm. Details of the growth procedure as well as the results of the conventional characterizations could be found in [14]. For XPS study a PHI 5000 VersaProbe spectrometer with monochromatic Al K α radiation ($h\nu = 1486.6$ eV) was used. The HR XPS spectra were collected with the hemispherical analyzer at the pass energy of 23.5 eV, the energy step size of 0.1 eV and the photoelectron take off angle of 45° with respect to the surface plane. The elemental bulk distribution was analyzed using the XPS technique combined with Ar⁺ depth profile sputtering with the following specifications: Ar⁺ ion source operates with the 0.5 kV Ar⁺ beam energy, the incident Ar⁺ ion beam axis is directed at 35° to the surface plane, the sputter area is 2×2 mm², argon ion beam current is 390 nA. The calibration performed on a 150 nm thick SiO₂/Si layer produced the sputter rate of 0.5 nm·min⁻¹. The sputter rate of metallic Nb or Si_{1-x}Nb_x alloy was not established due to lack of reference samples. Instead, the sputter rate of Nb was estimated from the measured sputter rate of a thick SiO₂ layer and the ratio 1.42 between etching rates of SiO₂ and Nb obtained at the same 0.5 kV Ar⁺ beam energy but higher beam current [25].

The surface charge compensation was achieved using a low energy electron flood gun. Binding energies of the photoelectrons were calibrated using the method described elsewhere [26]. The CasaXPS software (version 2.3.17) [27] was used to process the XPS data.

The decomposition procedure of the silicon data set started with a subtraction of a 'U 2 Tougaard' background. After that, the Si 2*p* spectra were deconvoluted taking the Gaussian-Lorentzian shape curves with 30% of Lorentzian character in order to determine the chemical nature of silicon states. Each silicon state was represented by Si 2*p*_{3/2} and Si 2*p*_{1/2} peaks separated by 0.63 eV. Following the model proposed by Himpsel et al. [28], four Si states can be clearly distinguished: the main state of the 2*p*_{3/2} line at binding energy (BE) of 99.2 eV is assigned to Si⁰ [29]. Three other states, which can be attributed to Si¹⁺, Si³⁺ and Si⁴⁺ suboxide states, are located at the distance of + 0.95, + 2.48 and + 3.9 eV from the Si⁰ line, respectively (see **Figure 1** (a)). Finally, a component corresponding to a mix phase of Si-Nb at the Si/Nb/Si interfaces was built exploiting the data presented by Matthew et al. [30], where

corresponding energy shift of silicon bounded to niobium line referred to Si^0 was estimated to be about - 0.5 eV.

As for the silicon data set, the decomposition procedure of the niobium data set started with a subtraction of a ‘U 2 Tougaard’ background. It is worth mentioning that there is a distribution of unfilled one-electron levels (conduction electrons) for niobium which are available for shake-up like events following the core electron photoemission. Consequently, instead of a discrete structure seen for shake-up satellites, a tail on the higher binding energy side of the main peak, manifested in an asymmetric peak shape, is observed [21, 31]. An example is shown in **Figure 1** (b). Thus, taking into account metallic nature of niobium the fit of Nb $3d$ doublet, for both samples, was done using two Lorentzian Asymmetric line shapes LA(1,3,5) and LA(1,2,5), respectively. A spin-orbit splitting of 2.72 eV and the peaks ratio 3:2 were utilized. Finally, a component corresponding to mix phase of Nb:Si was built using the value of + 0.6 eV as the corresponding energy shift referred to Nb^0 as it was estimated in [30].

3. Results and discussion

3.1. Thicker layer sample

Figures 1 (a),(b) and **2** (b),(d) clearly show that the 10 nm thick Si top layer does not prevent detection of Nb signal for a non-sputtered sample. This can be understood if an estimation of the “sampling depth” of photoelectrons that are detected by analyzer at a given set-up geometry is performed. Taking into account the incident beam energy (Al K_α radiation) and the nominal composition (pure Si layer), the depth of about 9.6 nm is needed to scatter 99% of all photoelectrons by the time they reach the surface [32]. One should not forget, however, that the oxidation of the silicon top layer is present, for which an inelastic mean free path is approximately 6.6 Å longer than for pure silicon. This allowed us to resolve the issue of the Nb $3d$ line visibility even before sputtering procedure and still to use the nominal thickness value (i.e. 10 nm) as the real value of the silicon top layer.

The analysis of Si $2p$ spectra for a non-sputtered sample presented in **Figures 1** (a), **2** (a), (b) indicates a presence of oxygen contamination at the surface of the silicon top layer. Si^0 state is identified at BE of the $2p_{3/2}$ line at 99.2 eV (according to [29]). Further analysis using the model proposed in [28] allowed identification of Si_2O (Si^{1+} at BE of 100.15 eV), Si_2O_3 (Si^{3+} at BE of 101.68 eV), and SiO_2 (Si^{4+} at BE of 103.1 eV) species.

Within the first few minutes of sputtering the silicon sub-oxide layer is removed (see **Figures 2** (a), (b)). At the same time, during the first 12 min, the position of $\text{Si}^0 2p$ line stays at the same BE (± 0.1 eV).

As for the Nb $3d$ line, for a non-sputtered sample and during first 7 min of sputtering, it was found to be comprised of a doublet at 202.2 eV and 204.9 eV corresponding to niobium species ($3d_{5/2} \text{Nb}^0$: 202.2 eV [33, 34]) (see **Figures 2** (c), (d)). The existence of oxide species of Nb, such as Nb^{2+} (+ 2 eV), Nb^{4+} (+ 4 eV), and Nb^{5+} (+ 5.5 eV) identified from the XPS spectra in [35], was not confirmed throughout this experiment.

At 12 minutes of sputtering, we estimate that approximately 6 nm of the Si top layer was removed. Further sputtering introduces drastic changes to the behavior of Si $2p$ and Nb $3d$ lines. The Si $2p$ line starts to shift to lower BEs. At the same time (12 min of sputtering), a major Nb $3d_{5/2}$ peak at 202.83 eV is assigned to niobium bounded to silicon close to the top of Si/Nb interface. A small shoulder at about 202.23 eV, which corresponds to metallic Nb^0 component, starts to increase significantly after further sputtering and reaches maximum at approximately 21 min of sputtering, i.e. pure Nb signal is seen in the data set (see **Figures 2** (c), (d)). Such modification of silicon and niobium electronic states is associated with the destruction of the originally sharp/pure interface, so that silicon atoms from the top layer and niobium atoms are mixed, thus, forming $\text{Si}_x\text{Nb}_{1-x}$ alloy close to the interface region/s.

It is worth noting that the estimated values of BEs obtained for Si and Nb agree well with the results presented for the amorphous $\text{Nb}_x\text{Si}_{1-x}$ alloys [30].

From approximately 25 min of sputtering, the Si $2p$ line starts to move back to higher BEs while the peak corresponding to metallic niobium, Nb^0 , disappears completely after 33 min of sputtering (see **Figures 2** (a)-(d)). Such changes indicate the formation of $\text{Si}_{1-x}\text{Nb}_x$ alloy rich in silicon.

Further sputtering, until up to 50 min or even more, does not completely remove Nb from the system, which allows us to conclude that Nb atoms from originally pure layer were pushed to Si bottom layer during sputtering process where they now form a $\text{Si}_{1-x}\text{Nb}_x$ area.

Eventually, long sputtering of approximately 50 min clearly shows penetration into glass substrate. A signal, which corresponds to a diffusion of oxygen from the substrate into a silicon bottom layer, is observed in the region 50-40 mins of sputtering.

Figures 2 (e), (f) contain the contour plots of valence band region as a function of sputtering time, along with selected XPS valence band spectra. As can be noticed, the position of a VB feature at lower BE we assign with Nb $4d$ states: it shifts to 1.8 eV and reaches maximum for

21 min of sputtering. Let us note that the feature around 9 eV in the VB XPS spectra indicates the position of the Si 3s electrons and it was shown [20] that intensity rises with increasing Si concentration in Si_{1-x}Nb_x layer. No feature corresponding to Si 3s states can be observed after 21 min of sputtering but then appears again after approximately 30 min of sputtering. This allows us to confirm our hypothesis made from the XPS data analysis: a pure niobium core exists and sputtering intermixes severely atoms Si and Nb.

3.2. Thinner layer sample

As in the case of the thicker layer sample, a non-sputtered thinner sample showed oxygen contamination at the surface of the silicon top layer. The same Si⁰, Si₂O (Si¹⁺), Si₂O₃ (Si³⁺), and SiO₂ (Si⁴⁺) states were identified with the same BEs.

After quick removal of the silicon sub-oxide layer, sputtering up to 25 min does not produce such drastic changes to the Si 2p line or to the Nb 3d line as in the case of the thicker layer sample. The effect of a pronounced shift of the Si 2p line to lower BEs is not clearly visible on the contour plot for the thinner layer sample, and the signal corresponding to Si-Nb species is observed (see **Figures 3** (a), (b)). From the positions of the Nb 3d_{5/2} peak before (202.55 eV) and after (202.75 eV) sputtering (see **Figures 3** (c), (d)), one can conclude that, together with the absence of the metallic Nb⁰ component (202.2 eV), Si_xNb_{1-x} species have been formed within the top interface *or/and* Nb interlayer. Quick estimation of the composition from the results obtained for the amorphous Nb_xSi_{1-x} alloys [30], allowed us to conclude that an alloy with niobium content of about 90 at.% is present at the top interface. The results of the comprehensive analysis utilizing SESSA software agree well with this estimated composition [36].

Further sputtering in the period of 25 - 33 min reveals a diffusion of oxygen from the substrate to silicon bottom layer as a contribution from two different species of oxides was discovered in the Si 2p signal (O 1s spectra are not presented here).

Finally, long sputtering of approximately 35 min or more not only shows that penetration into glass substrate occurred but it shows also that there is a complete disappearance of a signal from Nb. This happened at much shorter sputtering time since nominal thickness of niobium layer is just 1.3 nm compared to 9.5 nm for the thicker layer sample.

Figures 3 (e), (f) contain the contour plots of valence band region as a function of sputtering time, along with selected XPS valence band spectra. The position of VB maximum is about 2.1 eV (17 min of sputtering), but position of the feature around 9 eV remains unchanged after and

before sputtering procedure (marked by arrow). That feature indicates the position of the Si 3s electrons, as was shown in [20], its intensity rises with increasing Si concentration in $\text{Si}_{1-x}\text{Nb}_x$. Generally, subsequent sputtering manifests different behavior of valence density of state in the thicker layer sample as compared to the thinner layer sample. For both of them there is a clear evidence of Nb 4d states rising as a function of sputtering. VB FWHM value for the thicker layer sample is narrower compared to the thinner layer one, which highlights the higher contribution of Si 3p – Nb 4d mixed states for the latter. Finally, no feature corresponding to Si 3s states can be observed for the thicker layer sample after 21 min of sputtering, as opposed to the case of the thinner layer sample: Si 3s states are always there. All above allows us to confirm our hypothesis made from the XPS data analysis: a pure niobium core exists in the thicker layer sample as opposed to the thinner layer sample which contains $\text{Si}_{1-x}\text{Nb}_x$ rather than pure niobium layer.

4. Conclusions

Ultrathin Si/Nb/Si trilayer system with 9.5 and 1.3 nm thick niobium layer buried in amorphous silicon prepared by magnetron sputtering was studied using XPS depth-profiling technique. The results of the analysis of the Nb 3d, Si 2p HR XPS spectra clearly show a strong modification of electronic structure during argon sputtering procedure. Nevertheless, the information on an electronic structure of the interface and interface's sharpness, as a function of niobium layer thickness was successfully extracted. A sharp top interface and metallic phase of niobium were detected for the thicker layer sample. On the contrary, a Nb-rich mixed alloy at top interface was observed for the thinner layer sample.

Let us also note that the exploitation of XPS depth-profiling technique should be accompanied with realization that sputtering procedure can seriously affect the interlayer structure. If available, a preference should be given to synchrotron light source since it makes possible probing of XPS signal depth simply by tuning the excitation energy instead of sputtering. In addition, decrease of the uncertainties of the measured signal intensity would enhance a depth profile quality.

Acknowledgments

The authors would like to thank dr. W. Lisowski from the Institute of Physical Chemistry PAS (Warsaw, Poland) for the XPS measurements, dr. L. Y. Zhu from the Johns Hopkins

University (Maryland, USA) for the samples preparation. We acknowledge also the support from EAgLE project (Project Number: 316014).

References

- [1] I. Zaytseva, M.Z. Cieplak, A. Abal'oshev, P. Dluzewski, G. Grabecki, W. Plesiewicz, L.Y. Zhu, C.L. Chien, Magnetoresistance of Si/Nb/Si Trilayers, *Acta Phys. Polon. A*, 118 (2010) 406-408.
- [2] A.F. Mayadas, R.B. Laibowitz, J.J. Cuomo, Electrical Characteristics of rf Sputtered Single Crystal Niobium Films, *J. Appl. Phys.* 43 (1972) 1287-1289.
- [3] J.H. Quateman, TC Suppression and Critical Fields in Thin Superconducting Nb Films, *Phys. Rev. B* 34 (1986) 1948-1951.
- [4] S.I. Park, T.H. Geballe, Superconducting Tunneling in Ultrathin Nb Films, *Phys. Rev. Lett.* 57 (1986) 901-904.
- [5] J.W.P. Hsu, A. Kapitulnik, Superconducting Transition, Fluctuation, and Vortex Motion in a Two-Dimensional Single-Crystal Nb Film, *Phys. Rev. B* 45 (1992) 4819-4835.
- [6] K. Yoshii, H. Yamamoto, K. Saiki, A. Koma, Superconductivity and Electrical Properties in Single-Crystalline Ultrathin Nb Films Grown by Molecular-Beam Epitaxy, *Phys. Rev. B* 52 (1995) 13570-13575.
- [7] A.I. Gubin, K.S. Il'in, S.A. Vitusevich, M. Siegel, N. Klein, Dependence of Magnetic Penetration Depth on the Thickness of Superconducting Nb Thin Films, *Phys. Rev. B* 72 (2005) 064503.
- [8] T.R. Lemberger, I. Hetel, J.W. Knepper, F.Y. Yang, Penetration Depth Study of Very Thin Superconducting Nb Films, *Phys. Rev. B* 76 (2007) 094515.
- [9] E. Bemporad, F. Carassiti, M. Sebastiani, G. Lanza, V. Palmieri, H. Padamsee, Superconducting and Microstructural Studies on Sputtered Niobium Thin Films for Accelerating Cavity Applications, *Supercond. Sci. Technol.* 21 (2008) 125026.
- [10] C. Delacour, L. Ortega, M. Faucher, T. Crozes, T. Fournier, B. Pannetier, V. Bouchiat, Persistence of Superconductivity in Niobium Ultrathin Films Grown on R-plane Sapphire, *Phys. Rev. B* 83 (2011) 144504.

- [11] M. Salvato, M. Lucci, I. Ottaviani, M. Cirillo, N. Behabtu, C.C. Young, M. Pasquali, A. Vecchione, R. Fittipaldi, V. Corato, Superconductive Niobium Films Coating Carbon Nanotube Fibers, *Supercond. Sci. Technol.* 27 (2014) 115006.
- [12] G. Pristáš, S. Gabáni, M. Orendáč, V. Komanický, E. Gažo, Study of Niobium Thin Films under Pressure, *Acta Phys. Pol. A* 126 (2014) 346-347.
- [13] M.I. Tsindlekht, V.M. Genkin, I. Felner, F. Zeides, N. Katz, Š. Gazi, Š. Chromik, dc and ac Magnetic Properties of Thin-Walled Superconducting Niobium Cylinders, *Phys. Rev. B* 90 (2014) 014514.
- [14] I. Zaytseva, O. Abal'oshev, P. Dłużewski, W. Paszkowicz, L.Y. Zhu, C.L. Chien, M. Kończykowski, M.Z. Cieplak, Negative Hall Coefficient of Ultrathin Niobium in Si/Nb/Si Trilayers, *Phys. Rev. B* 90 (2014) 060505(R).
- [15] I. Zaytseva, O. Abal'oshev, P. Dłużewski, R. Minikayev, M.Z. Cieplak, L.Y. Zhu, C.L. Chien, Ultrathin Niobium in the Si/Nb/Si Trilayers, *Acta Phys. Pol. A* 126 (2014) A-140-A-144.
- [16] K. Söldner, A. Grassmann, G. Saemann-Ischenko, W. Zahorowski, A. Šimůnek, G. Wiech, Electronic Structure of Amorphous Nb_{1-x}Si_x Films Studied by X-ray Emission and X-ray Photoelectron Spectroscopy, *Z. Phys. B: Condens. Matter* 75 (1989) 59-65.
- [17] G. Wiech, W. Zahorowski, A. Šimunek, O. Siper, On the Bonding and Structure of Amorphous Nb_{1-x}Si_x Films, *J. Phys.: Condens. Matter* 1 (1989) 5595-5606.
- [18] P.J.W. Weijs, H. van Leuken, R.A. de Groot, J.C. Fuggle, S. Reiter, G. Wiech, K.H.J. Buschow, X-ray-Emission Studies of Chemical Bonding in Transition-Metal Silicides, *Phys. Rev. B* 44 (1991) 8195-8203.
- [19] P.K. Hucknall, C.G.H. Walker, D. Greig, J.A.D. Matthew, D. Norman, J. Turton, Detailed Studies of the Density of States of Amorphous NbSi Obtained by Synchrotron Radiation Photoemission, *J. Phys.: Condens. Matter* 4 (1992) 1131-1141.
- [20] K. Söldner, G. Saemann-Ischenko, Correlation Between Transport Properties and Valence Band Spectra of Thin Films of Nb_{1-x}Si_x, *Jap. J. of Appl. Phys.* 26 (1987) 807-808.

- [21] D. Briggs, XPS: Basic Principles, Spectral Features and Qualitative Analysis; published in Surface Analysis by Auger and X-ray Photoelectron Spectroscopy (Eds. D. Briggs and J.T. Grant), IM Publications: Chichester, 2003, pp. 31-56.
- [22] N.Q. Lam, Ion bombardment effects on the near-surface composition during sputter profiling, Surf. Interface Anal. 12 (1988) 65-77.
- [23] S. Hofmann, Sputter depth profile analysis of interfaces, Rep. Prog. Phys. 61 (1998) 827-888.
- [24] S. Oswald, R. Reiche, Binding state information from XPS depth profiling: capabilities and limits, Appl. Surf. Sci. 179 (2001) 307-315.
- [25] Etch Rates of Selected Materials. Microfab, Inc., http://www.microfabnh.com/ion_beam_etch_rates.php (accessed May 01, 2016).
- [26] K. Asami, A Precisely Consistent Energy Calibration Method for X-ray Photoelectron Spectroscopy, J. Electron Spectrosc. Relat. Phenom. 9 (1976) 469-478.
- [27] N. Fairley, Casa Software Ltd, Software Package for the Analysis of XPS Results, CasaXPS version 2.3.17dev6.6o, <http://www.casaxps.com>.
- [28] F.J. Himpsel, F.R. McFeely, A. Taleb-Ibrahimi, J. A. Yarmoff, G. Hollinger, Microscopic Structure of the SiO₂/Si Interface, Phys. Rev. B 38 (1988) 6084-6096.
- [29] C.D. Wagner, Photoelectron and Auger Energies and the Auger Parameter: A Data Set; published in Practical Surface Analysis, Vol. 1. Auger and Photoelectron Spectroscopy (Eds. D. Briggs and M.P. Seah); Wiley: New York, 1990, pp. 595-625.
- [30] J.A.D. Matthew, S.A. Morton, C.G.H. Walker, G. Beamson, Auger Parameter Studies of Amorphous NbSi, J. Phys. D: Appl. Phys. 28 (1995) 1702-1706.
- [31] M.C. Biesinger, L.W.M. Lau, A.R. Gerson, R.St.C. Smart, Resolving Surface Chemical States in XPS Analysis of First Row Transition Metals, Oxides and Hydroxides: Sc, Ti, V, Cu and Zn, Appl. Surf. Sci. 257 (2010) 887-898.
- [32] C.J. Powell, A. Jablonski, NIST Electron Effective-Absorption-Length Database, National Institute of Standards and Technology: Gaithersburg, MD, 2011.

- [33] I. Arfaoui, J. Cousty, C. Guillot, A Model of the $\text{NbO}_{x \approx 1}$ Nanocrystals Tiling a Nb(110) Surface Annealing in UHV, *Surf. Sci.* 557 (2004) 119-128.
- [34] A.S. Razinkin, Oxide Nanostructures on a Nb Surface (110): XPS-, XRD-, and STM Investigations (Ph.D. thesis); Ekaterinburg, Russia, 2009.
- [35] F.L. Palmer, Influence of Oxide Layers on the Microwave Surface Resistance of Superconducting Niobium (Ph.D. thesis); Cornell University, U.S.A., 1988.
- [36] I.N. Demchenko, W. Lisowski, Y. Syryanny, Y. Melikhov, I. Zaytseva, P. Konstantynov, M. Chernyshova, M.Z. Cieplak, Use of XPS to clarify the Hall coefficient sign variation in thin niobium layers buried in silicon, *Appl. Surf. Sci.* 399 (2017) 32-40.

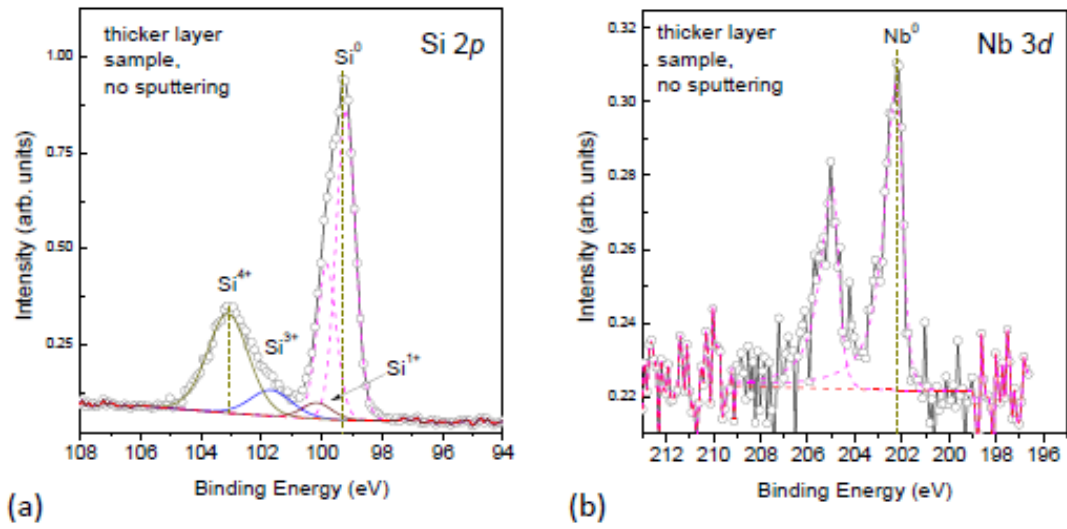


Figure 1. (color online) XPS spectra of the (a) Si 2p and (b) Nb 3d regions for the thicker layer sample before sputtering. Reminder: nominal thickness of the top and bottom silicon layers is about 10 nm with the nominal thickness of niobium film of about 9.5 nm.

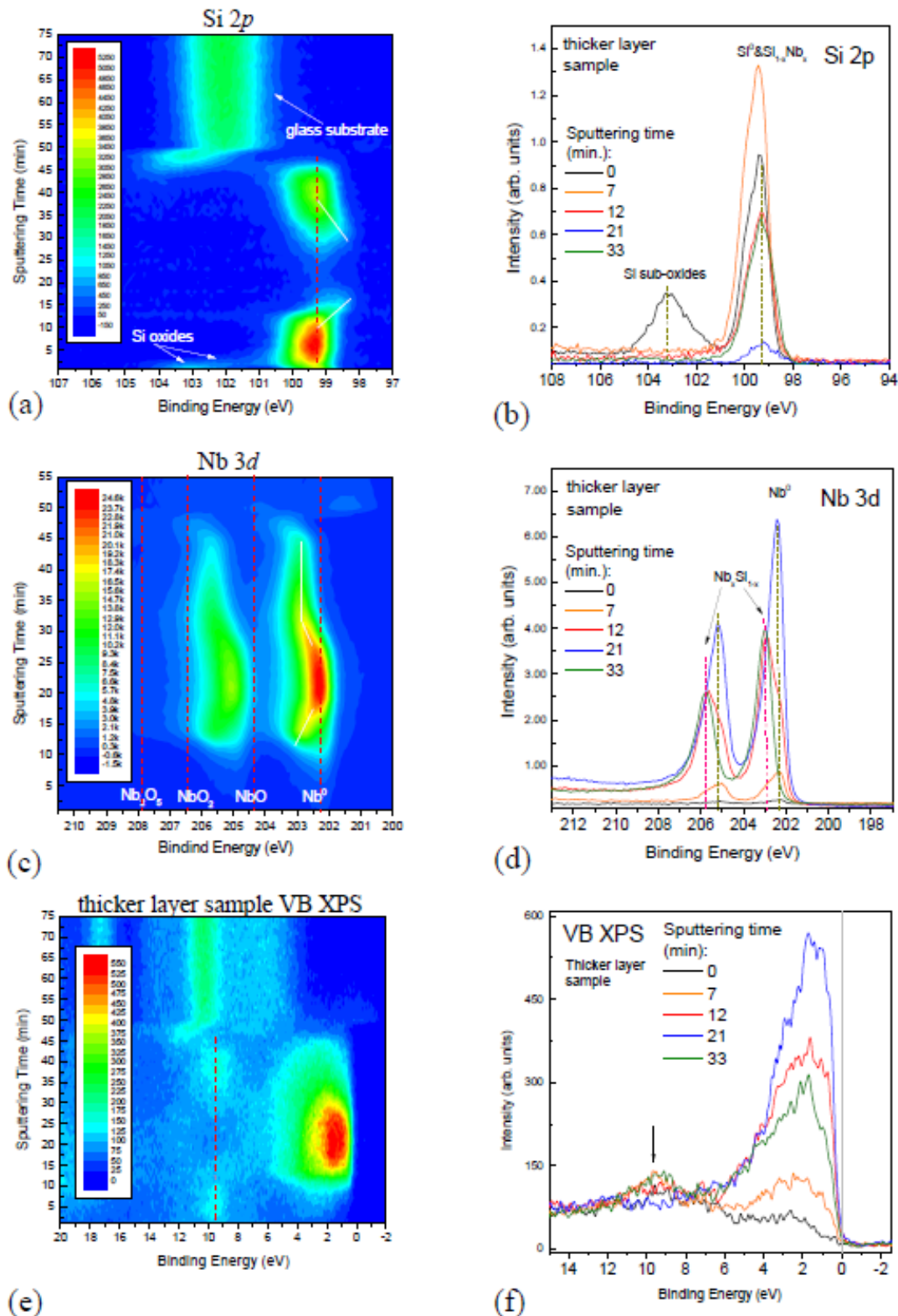


Figure 2. (color online) Experimental XPS results for the thicker layer sample: Si 2*p* line (a) contour plot and (b) spectra for selected sputtering minutes; Nb 3*d* line (c) contour plot with marked positions of Nb 3*d*_{5/2} line of Nb⁰, NbO (Nb²⁺), NbO₂ (Nb⁴⁺), and Nb₂O₅ (Nb⁵⁺) and (d) spectra for selected sputtering minutes; XPS valence band (VB XPS) region (e) contour plot and (f) spectra for selected sputtering minutes.

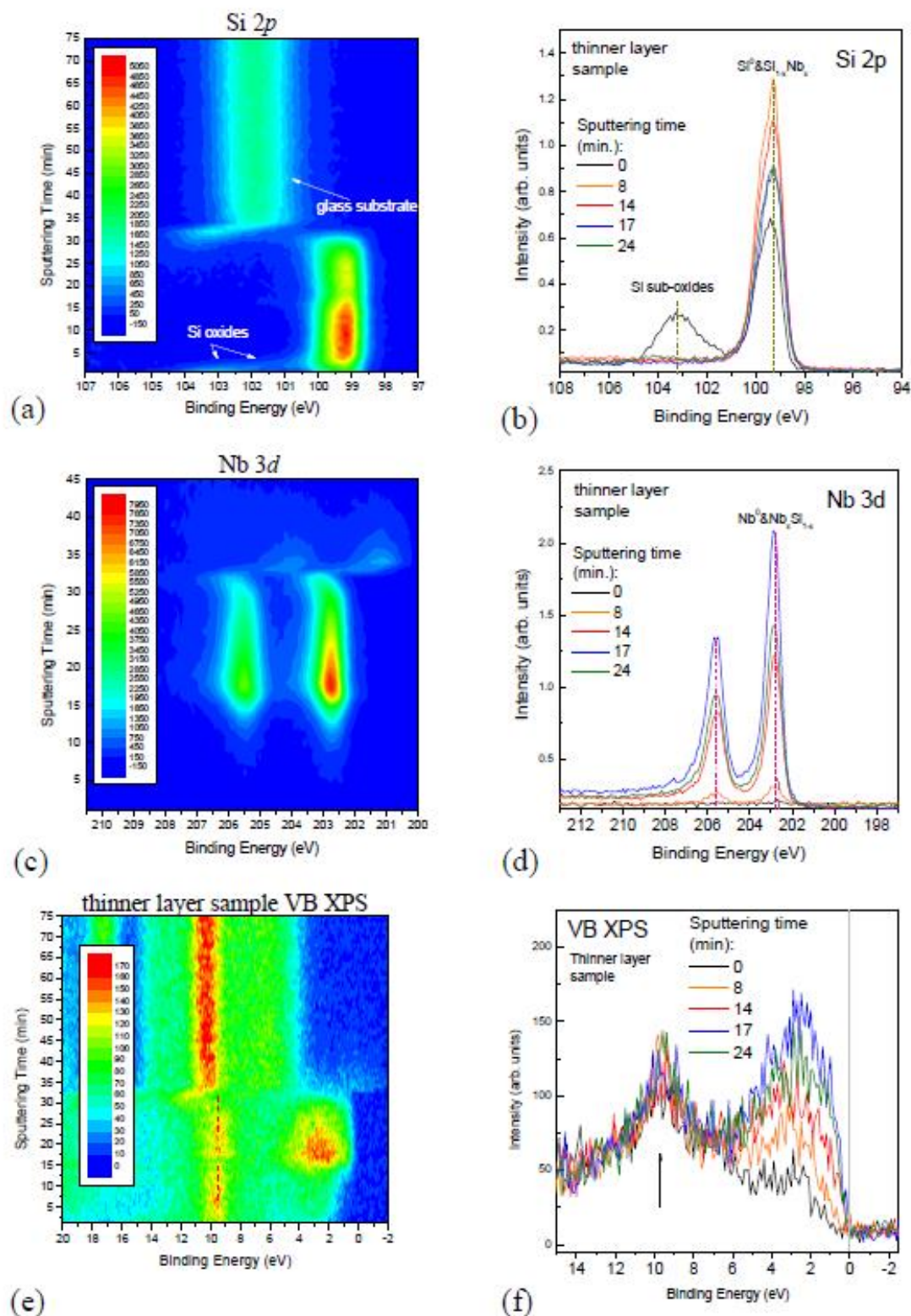


Figure 3. (color online) Experimental XPS results for the thinner layer sample: Si 2*p* line (a) contour plot and (b) spectra for selected sputtering minutes; Nb 3*d* line (c) contour plot and (d) spectra for selected sputtering minutes; VB XPS region (e) contour plot and (f) spectra for selected sputtering minutes.